J|A|C|S ARTICLES

Published on Web 03/31/2010

Uncovering the Design Rules for Peptide Synthesis of Metal Nanoparticles

Yen Nee Tan,[‡] Jim Yang Lee,*[,†,‡] and Daniel I. C. Wang[‡,§]

Department of Chemical and Biomolecular Engineering, National University of Singapore, 10 Kent Ridge Crescent, Singapore 119260, Singapore−MIT Alliance, 4 Engineering Drive 3, National University of Singapore, Singapore 117576, and Department of Chemical Engineering, Massachusetts Institute of Technology, 77 Massachusetts Avenue, Room 16-429, Cambridge, Massachusetts 02139

Received September 3, 2009; E-mail: cheleejy@nus.edu.sg

Abstract: Peptides are multifunctional reagents (reducing and capping agents) that can be used for the synthesis of biocompatible metal nanoparticles under relatively mild conditions. However, the progress in peptide synthesis of metal nanoparticles has been slow due to the lack of peptide design rules. It is difficult to establish sequence−reactivity relationships from peptides isolated from biological sources (e.g., biomineralizing organisms) or selected by combinatorial display libraries because of their widely varying compositions and structures. The abundance of random and inactive amino acid sequences in the peptides also increases the difficulty in knowledge extraction. In this study, a "bottom-up" approach was used to formulate a set of rudimentary rules for the size- and shape-controlled peptide synthesis of gold nanoparticles from the properties of the 20 natural α-amino acids for $AuCl_4^-$ reduction and binding to Au^0. It was discovered that the reduction capability of a peptide depends on the presence of certain reducing amino acid residues, whose activity may be regulated by neighboring residues with different Au^0 binding strengths. Another finding is the effect of peptide net charge on the nucleation and growth of the Au nanoparticles. On the basis of these understandings, several multifunctional peptides were designed to synthesize gold nanoparticles in different morphologies (nanospheres and nanoplates) and with sizes tunable by the strategic placement of selected amino acid residues in the peptide sequence. The methodology presented here and the findings are useful for establishing the scientific basis for the rational design of peptides for the synthesis of metal nanostructures.

Introduction

Metal nanoparticles are finding increasing acceptance in biomedical applications. Gold nanoparticles, in particular, are useful for biosensing,[1−4] bioimaging,[2,5] drug and gene delivery,[6] and cancer photothermal therapy.[7,8] The versatility of gold nanoparticles is due in large part to their unique surface plasmon resonance (SPR) properties which may be varied through particle size and shape manipulations.[9−13] However, the synthesis of metal nanoparticles by chemical means often requires the use of harsh reagents (e.g., cetyltrimethylammonium bromide, CTAB) and sometimes organic solvents (e.g., toluene) for particle morphology (i.e., size and shape) control.[12−15] The remaining presence of harsh chemicals in the final product is clearly unacceptable for biomedical applications,[16−18] necessitating the search for benign alternatives to chemical synthesis.[19] The use of proteins and/or peptides for metal nanoparticles synthesis is ideal in this respect because of the assured

[†] National University of Singapore.
[‡] Singapore−MIT Alliance.
[§] Massachusetts Institute of Technology.

(1) Anker, J. N.; Hall, W. P.; Lyandres, O.; Shah, N. C.; Zhao, J.; van Duyne, R. P. *Nat. Mater.* **2008**, *7*, 442–453.
(2) Murphy, C. J.; Gole, A. M.; Hunyadi, S. E.; Stone, J. W.; Sisco, P. N.; Alkilany, A.; Kinard, B. E.; Hankins, P. *Chem. Commun.* **2008**, 544–557.
(3) Thaxton, C. S.; Georganopoulou, D. G.; Mirkin, C. A. *Clin. Chim. Acta* **2006**, *363*, 120–126.
(4) Sepúlveda, B.; Angelomé, P. C.; Lechuga, L. M.; Liz-Marzán, L. M. *Nano Today* **2009**, *4*, 244–251.
(5) Hu, M.; Chen, J.; Zhi-Yuan, L.; Leslie, A.; V, H. G.; Li, X.; Manuel, M.; Xia, Y. *Chem. Soc. Rev.* **2006**, *35*, 1084–1094.
(6) Ghosha, P.; Hana, G.; Dea, M.; Kima, C. K.; Rotello, V. M. *Adv. Drug Delivery Rev.* **2008**, *60*, 1307–1315.
(7) Huang, X. H.; Jain, P. K.; El-Sayed, I. H.; El-Sayed, M. A. *Nanomedicine* **2007**, *2*, 681–693.
(8) Jain, P. K.; El-Sayed, I. H.; El-Sayed, M. A. *Nano Today* **2007**, *2*, 18–29.
(9) Burda, C.; Chen, X. B.; Narayanan, R.; El-Sayed, M. A. *Chem. Rev.* **2005**, *105*, 1025–1102.
(10) Eustis, S.; El-Sayed, M. A. *Chem. Soc. Rev.* **2006**, *35*, 209–217.
(11) Orendorff, C. J.; Sau, T. K.; Murphy, C. J. *Small* **2006**, *2*, 636–639.
(12) Murphy, C. J.; Sau, T. K.; Gole, A. M.; Orendorff, C. J.; Gao, J.; Gou, L.; Hunyadi, S. E.; Li, T. *J. Phys. Chem. B* **2005**, *109*, 13857–13870.
(13) Tao, A. R.; Habas, S.; Yang, P. *Small* **2008**, *4*, 310–325.
(14) Zhang, Q.; Xie, J.; Liang, J.; Lee, J. Y. *Adv. Funct. Mater.* **2009**, *19*, 1387–1398.
(15) Grzelczak, M.; Pérez-Juste, J.; Mulvaney, P.; Liz-Marzán, L. M. *Chem. Soc. Rev.* **2008**, *37*, 1783–1791.
(16) Wang, S.; Lu, W.; Tovmachenko, O.; Rai, U. S.; Yu, H.; Ray, P. C. *Chem. Phys. Lett.* **2008**, *463*, 145–149.
(17) Connor, E. E.; Mwamuka, J.; Gole, A.; Murphy, C. J.; Wyatt, M. D. *Small* **2005**, *1*, 325–327.
(18) Alkilany, A. M.; Nagaria, P.; Hexel, C. R.; Shaw, T. J.; Murphy, C. J. *Small* **2009**, *5*, 701–708.
(19) Hutchison, J. E. *ACS Nano* **2008**, *2*, 395–402.

biocompatibility and the reduced environmental footprint of carrying out the synthesis at room temperature and at or near neutral pH in aqueous solution. Additionally, the large diversity of proteins and/or peptides available for use and exploration offers a new opportunity to organize, interact, and direct the shape, size, and structure evolution of the metal nanoparticles in more varied and innovative ways.

The use of proteins and peptides for the *in vitro* production of metal nanoparticles is inspired by the roles of these biomolecules in natural biomineralization.[20,21] The most direct way to produce biomolecules suitable for *in vitro* materials synthesis is to extract the proteins or peptides from biomineralizing organisms. This is generally known as the "top-down" or the "reductionist" approach.[22−24] Multistep processing is required, involving invariably the isolation, purification, and cloning of specific proteins. This top-down approach is therefore a complex, labor-intensive, and time-demanding operation. The active proteins are often a minor component amidst the myriad of proteins recovered; they also vary widely in composition and structure because of their different origins. This has presented significant problems for the analysis and identification of the active proteins and the establishment of protein sequence−reactivity relationships. Recently, combinatorial screening methods such as phage display (PD) and cell surface display (CSD) techniques have been used for selecting peptide sequences that bind specifically to inorganic (e.g., metal) surfaces.[25−31] In some cases these peptides also show the capability to reduce metal ions and to template the crystal growth of the metal nanoparticles.[29−31] For example, Naik et al.[30] found that two of the three PD-selected silver-binding peptides can be used to synthesize a variety of silver nanoparticles (including spherical nanoparticles and triangular and hexagonal nanoplates) without any exogenous reducing agent. However, such bioprospecting efforts provide relatively little insight into how molecular details such as the peptide amino acid composition and sequence would impact the metal nanoparticle synthesis.

Peptides that have been identified through the traditional top-down approach or the modern combinatorial approach are not useful for the development of design rules for metal nanoparticle synthesis. This is because these peptides are diversely different in composition and contain embedded random and inactive amino acid sequences. While amino acids provide a basic working set for metal nanoparticle synthesis, a prudent combination of the selected amino acids is required to form a functional protein/peptide. This has motivated us to explore the "bottom-up" alternative, where the various required functionalities of a peptide may be assembled from the basic protein building blocks in a principled way. This study, using gold as a model system, started with the identification of the functions of the 20 natural α-amino acids in chloroaurate reduction and binding to elemental gold. This was followed by the investigation of the interactions between these functionalities when the amino acids are assembled into short peptide sequences for Au nanocrystals formation and growth. Through an elaborate experimental effort, we have formulated several peptide design rules by the bottom-up approach and demonstrated their use in the morphosynthesis of gold nanoparticles with artificially crafted peptides designed on the basis of these rules.

Results and Discussion

Similar to conventional metal nanoparticle synthesis, the formation of metal nanoparticles by proteins or peptides requires two basic functionalities, i.e., reduction capability for metal ions and capping capability for the nanoparticles formed. Since proteins are constituted from amino acids, their activity in metal nanoparticle synthesis must be related to the presence of certain amino acid residues in a peptide sequence. Indeed, several independent studies have shown that some amino acids could be used as the reductant and/or capping agent in metal nanoparticle synthesis.[32−37] However, no systematic study was carried out to screen the reduction and binding capabilities of the 20 natural α-amino acids[38] or to investigate the effect of amino acid sequence in the peptide synthesis of metal nanoparticles. Presented below are the details of this investigation to address this missing information, using gold as a model system.

Reduction Capability Studies. The reduction capabilities of the 20 amino acids were studied under the same reaction conditions and ranked by the time taken to transform the yellowish gold precursor solution ($HAuCl_4$) into the pinkish red-gold nanoparticle solution. Among the 20 amino acids, tryptophan (W) was found to be the fastest reducing agent (Table S1, middle column, Supporting Information). It was thus selected as the common reducing residue for the next study involving amino acid mixtures. The aim of the mixture study was to determine how the presence of another amino acid in the mixture would affect the reduction rate. The results in Table S1 (right column) show that, for the majority of amino acid mixtures with W as a common constituent, the reduction kinetics was the *same* as that of tryptophan on its own. This suggests that the rate of reduction was determined mainly by the faster reducing agent (i.e., W) in the mixture, and the contribution from the other

(20) Crookes-Goodson, W. J.; Slocik, J. M.; Naik, R. R. *Chem. Soc. Rev.* **2008**, *37*, 2403–2412.
(21) Dickerson, M. B.; Sandhage, K. H.; Naik, R. R. *Chem. Rev.* **2008**, *108*, 4935–4978.
(22) Xie, J.; Lee, J. Y.; Wang, D. I. C.; Ting, Y. P. *Small* **2007**, *3*, 672–682.
(23) Shankar, S. S.; Rai, A.; Ankamwar, B.; Singh, A.; Ahmad, A.; Sastry, M. *Nat. Mater.* **2004**, *3*, 482–488.
(24) Sanghi, R.; Verma, P. *Bioresource Technol.* **2009**, *100*, 501–504.
(25) Sarikaya, M.; Tamerler, C.; Jen, A. K.-Y.; Schulten, K.; Baneyx, F. *Nat. Mater.* **2003**, *2*, 577–585.
(26) Sarikaya, M.; Tamerler, C.; Schwartz, D. T.; Baneyx, F. O. *Annu. Rev. Mater. Res.* **2004**, *34*, 373–408.
(27) Brown, S. *Nat. Biotechnol.* **1997**, *15*, 269–272.
(28) Peelle, B. R.; Krauland, E. M.; Wittrup, K. D.; Belcher, A. M. *Langmuir* **2005**, *21*, 6929–6933.
(29) Naik, R. R.; Jones, S. E. J.; Murray, C. J.; McAuliffe, J. C.; Vaia, R. A.; O., S. M. *Adv. Funct. Mater.* **2004**, *14*, 25–30.
(30) Naik, R. R.; Stringer, S. J.; Agarwal, G.; Jones, S. E.; Stone, M. O. *Nat. Mater.* **2002**, *1*, 169–172.
(31) Brown, S.; Sarikaya, M.; Johnson, E. *J. Mol. Biol.* **2000**, *299*, 725–735.
(32) Tan, Y. N.; Lee, J. Y.; Wang, D. I. C. *J. Phys. Chem. C* **2008**, *112*, 5463–5470.
(33) Selvakannan, P.; Mandal, S.; Phadtare, S.; Pasricha, R.; Sastry, M. *Langmuir* **2003**, *19*, 3545–3549.
(34) Selvakannan, P.; Mandal, S.; Phadtare, S.; Gole, A.; Pasricha, R.; Adyanthaya, S. D.; Sastry, M. *J. Colloid Interface Sci.* **2004**, *269*, 97–102.
(35) Selvakannan, P.; Swami, A.; Srisathiyanarayanan, D.; Shirude, P. S.; Pasricha, R.; Mandale, A. B.; Sastry, M. *Langmuir* **2004**, *20*, 7825–7836.
(36) Si, S.; Mandal, T. *Chem.−Eur. J.* **2007**, *13*, 3160–3168.
(37) Willett, R. L.; Baldwin, K. W.; West, K. W.; Pfeiffer, L. N. *Proc. Natl. Acad. Sci. U.S.A.* **2005**, *102*, 7817.
(38) The following one-letter abbreviations are used for the 20 natural α-amino acids (X): A, alanine; C, cysteine; D, aspartic acid; E, glutamic acid; F, phenylalanine; G, glycine; H, histidine; I, isoleucine; K, lysine; L, leucine; M, methionine; N, asparagine; P, proline; Q, glutamine; R, arginine; S, serine; T, threonine; V, valine; W, tryptophan; Y, tyrosine.

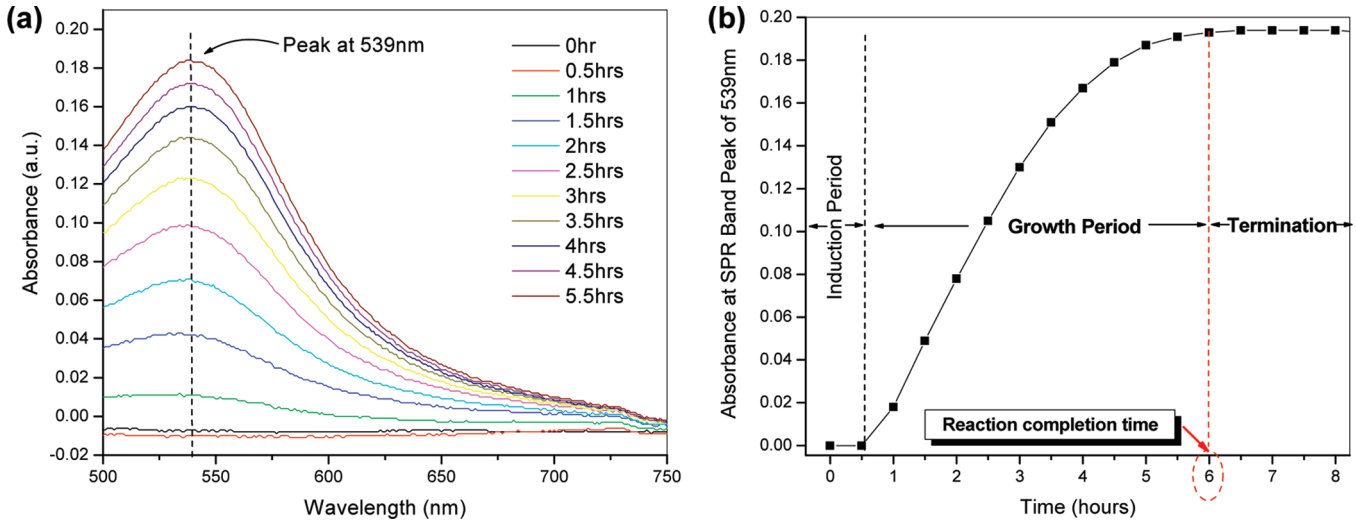

Figure 1. Kinetics of peptide (FWFWFWF) synthesis of gold nanoparticles. (a) Time-resolved UV−vis spectra focusing on the Au SPR spectral region. (b) Evolution of the SPR peak at 539 nm with time, showing three distinctive reaction regions.

amino acid with weaker reducing power was relatively minor. This is characteristic of a competing reaction system where the amino acids do not interact with each other. However, it is also important to consider the effect of metal ion complexation in reduction. Generally, complexation lowers the redox potential and hence the reducibility of the metal ions. Amino acids such as cysteine (C), histidine (H), and methionine (M) are known to form strong complexes with metal ions.[39] The observation of exceptionally slow reduction rates for the C−W, H−W, and M−W mixtures could be understood as such.

To examine the effects of a neighboring amino acid (X) on the reduction capability of W in a peptide sequence, tryptophan-interdigitated peptides (XWXWXWX) with the same overall amino acid compositions and W/X ratios as the amino acid mixture study were used. The kinetics of $AuCl_4^-$ ions reduction was monitored by the changes in the absorption maximum of the SPR of gold nanoparticles formed.[36,40−42] Figure 1a shows the UV−vis spectra of gold nanoparticles synthesized by the FWFWFWF peptide as an example. The time course of the absorbance at 539 nm (Figure 1b) has a characteristic sigmoidal shape consisting of three distinguishable reaction regimes: (I) the induction period, where the absorbance was low and visibly unchanged from the start of the reaction; (II) the growth period, where the absorbance underwent the most rapid changes; and (III) termination, where the SPR absorbance reached a plateau value signaling the end of the reaction. Similar sigmoidal curves were also obtained for the 20 W−X interdigitated peptide syntheses of gold nanoparticles (Figure S1, Supporting Information). The reduction capabilities of these peptides were likewise ranked by the time taken to completely reduce $AuCl_4^-$ (e.g., 6 h for FWFWFWF).

Comparing between the amino acid mixtures (green triangles) and peptides of the same overall composition (black squares) in Figure 2a, different trends of reduction capability were observed. When the amino acids with different reduction capabilities were homogenized in a well-mixed aqueous solution, the amino acids worked independently. The outcome was dominated by the amino acid that has the strongest interaction with the chloroaurate ions (either in the form of Au(III) reduction or complex formation). However, when the amino acids were connected to form a peptide sequence, the amino acid residues responded collectively to the reaction, resulting in vastly different kinetic behaviors. Hence, peptides are more effective and versatile than amino acid mixtures in manipulating the reduction kinetics in a nanoparticle synthesis. On the other hand, Figure 2b shows no direct correlation between the reduction capability of a pure amino acid and the reduction capability of the same amino acid when it was present in a peptide sequence. For example, tyrosine (Y), which showed fairly good reduction capability on its own (blue stars), actually downgraded the reactivity of W more than the other amino acids when it was incorporated as the W−Y sequence (black squares). Furthermore, tryptophan, which was the strongest reducing amino acid, did not show the best reduction capability when it was joined to form the WWWWWWW (W_7) homopeptide. These results indicate that *the reduction capability of a peptide is not the linear sum of the capabilities of its amino acid constituents*. The effects of different neighboring amino acids X on the reduction capability of W−X interdigitated peptides were investigated next to deduce some basic sequence−activity relationships.

Metal-Binding Affinity Measurements. Another equally important functionality of amino acid residues in a peptide sequence for Au nanoparticle synthesis is their binding interaction with the Au surface. For this we designed a series of interdigitated peptides that can be used to rank the relative binding affinities of the 20 amino acids. Surface plasmon resonance measurements were used to quantify the binding strengths of the interdigitated peptides on the gold surface. Since histidine (H) exhibits a strong binding interaction with gold,[43,44] it was used as a common binding residue in the XHXHXHX peptide sequence to sensitize the SPR detection and the comparison between different amino acid residues (X). The binding constants (K_A) of the peptides could be determined by

(39) Lippard, S. J.; Berg, J. M. *Principles of Bioinorganic Chemistry*; University Science Books: Mill Valley, CA, 1994.
(40) Santos, D. S.; Avarez-Puebal, R. A.; Oliveira, O. A.; Aroca, R. F. *J. Mater. Chem.* **2005**, *15*, 3045–3049.
(41) Cao, L.; Zhu, T.; Liu, Z. *J. Colloid Interface Sci.* **2006**, *293*, 69–76.
(42) Tan, Y. N.; Lee, J. Y.; Wang, D. I. C. *J. Phys. Chem. C.* **2009**, *113*, 10887–10895.
(43) Slocik, J. M.; Wright, D. W. *Biomacromolecules* **2003**, *4*, 1135–1141.
(44) Slocik, J. M.; Moore, J. T.; Wright, D. W. *Nano Lett.* **2002**, *2*, 169–173.

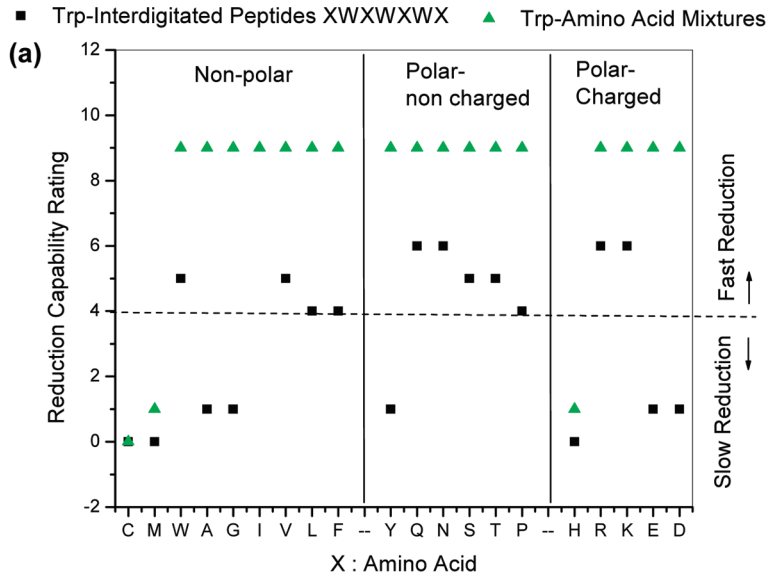

Reduction Rate Rating Scheme (I)

Time(hrs)	Rating
0 ~ 1	9
1 ~ 2	8
2 ~ 3	7
3 ~ 4	6
4 ~ 5	5
5 ~ 6	4
6 ~ 7	3
7 ~ 8	2
8 ~ 9	1
No reduction	0

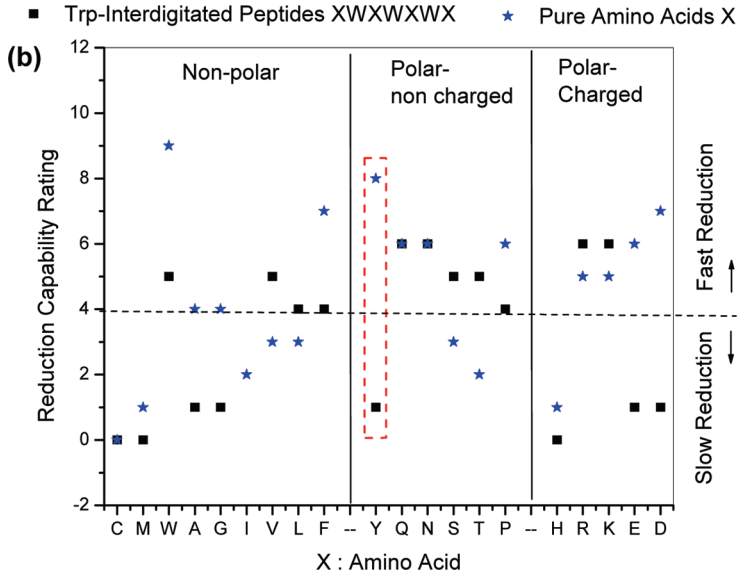

Reduction Rate Rating Scheme (II)

Time(hrs)	Rating
0 ~ 1	9
1 ~ 3	8
3 ~ 15	7
15 ~ 24	6
24 ~ 30	5
30 ~ 36	4
36 ~ 48	3
48 ~ 72	2
72 ~ 336	1
No reduction	0

Figure 2. Comparison of the reduction capabilities of (a) tryptophan-interdigitated peptides (XWXWXWX) (black squares) and tryptophan-containing (W−X) amino acid mixtures (green triangles), and (b) tryptophan-interdigitated peptides (black squares) and pure amino acids (X) (blue stars). Rating schemes for the reduction capability of (I) XWXWXWX peptides and (II) W−X amino acid mixtures and pure amino acids X.

fitting the SPR data to Langmuir isotherms[45] (details of the calculation method can be found in Figure S2, Supporting Information). Figure 3a shows the calculated binding constants of the 20 H−X interdigitated peptides, where a higher K_A value implies stronger binding on gold. To better visualize the binding behavior of peptides on the gold surface, the fractional surface coverages (θ) of the H−X interdigitated peptides at equilibrium were calculated from the following equation:[46]

$$\theta = \frac{R_{eq}}{R_{max}} = \frac{K_A C}{1 + K_A C} \quad (1)$$

The calculated results, as presented in Figure 3b, show that the peptide CHCHCHC covered the gold surface more extensively than other H−X interdigitated peptides at the same concentration. At low peptide concentrations (<0.1 mM), the equilibrium fractional surface coverage for the strongest binder, CHCHCHC, was about 30 times that of the weakest binder, PHPHPHP. This ratio decreased to about 4 at high concentrations (~1 mM) and would eventually reach unity at very high concentrations. The gradual decrease in the slope of the isotherm with concentration is expected, as the already-adsorbed peptide on the gold surface would increase the steric hindrance upon further adsorption. Hence, it is more meaningful to use the binding affinity measured at a low peptide concentration (0.1 mM) for the comparison of peptides. As such, the equilibrium surface coverage of a peptide on the gold surface normalized by that of QHQHQHQ (an intermediate binder) was used as a comparator of relative binding strengths, with a ratio >1 indicating strong binding and a ratio <1 indicating weak binding (Figure 3c). The results showed that H−X interdigitated peptides with amino acid residues containing nitrogen heterocycles (H,

(45) Karpovich, D. S.; Blanchard, G. J. *Langmuir* **1994**, *10*, 3315–3322.
(46) In the equation, C is the peptide concentration, R_{eq} is the binding level of peptide at the equilibrium (in response unit, RU); R_{max} is the maximum binding capacity of the peptide, and K_A is the binding constant.

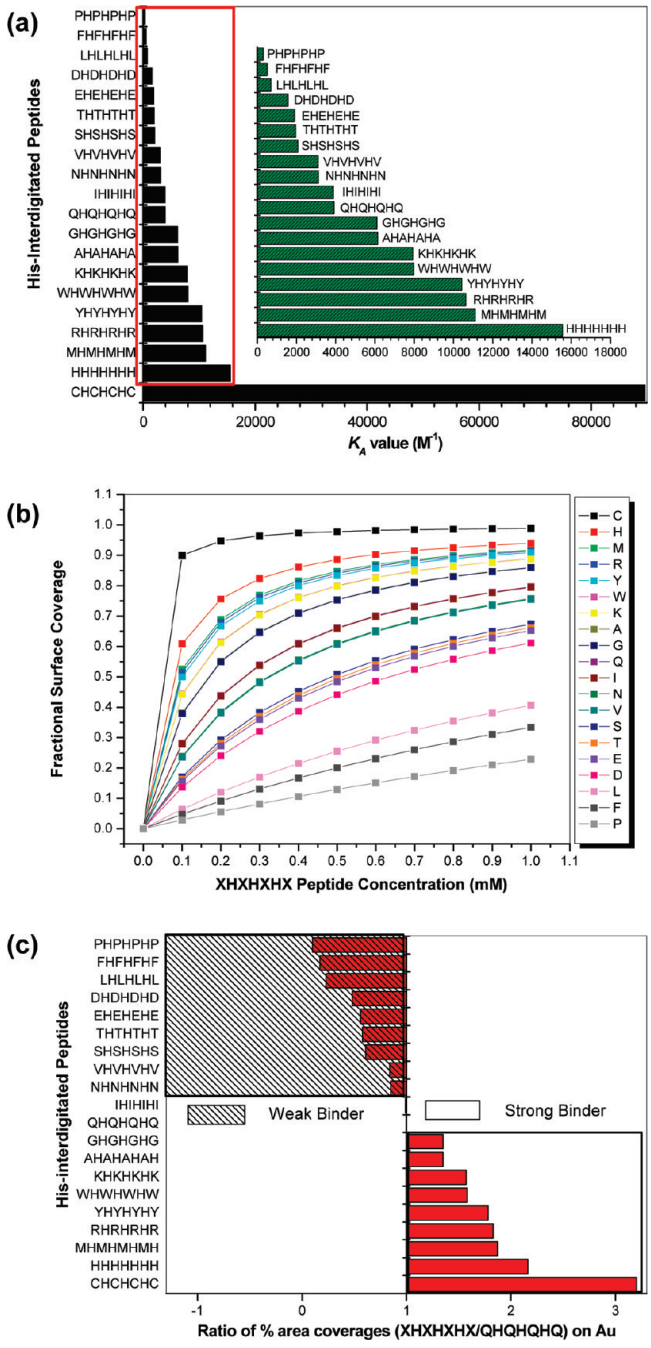

Figure 3. (a) K_A values of histidine-interdigitated peptides (XHXHXHX) on Au surface. The inset shows an expanded view of the red box on the left. (b) Fractional surface coverage of peptides on Au at different peptide concentrations. (c) Contextual representation of relative binding strength based on surface coverage normalized by that of QHQHQHQ on gold measured at the same 0.1 mM peptide concentration.

W) or sulfur (C, M) in their side chains are strong binders, whereas those with acidic and hydrophobic side chains without nitrogen are weak binders. Furthermore, binding affinity also increased with the increase in peptide conformational flexibility (i.e., G > Q > P). Glycine (G) and proline (P), which are unique in their influence on polypeptide conformation, strongly affected the interaction between the imidazole side chain of histidine and the gold surface. The simple glycine molecule with no side chain allowed the peptide to adapt easily to conformations favorable for binding to gold. In contrast, proline, being a rigid amino acid, had minimum flexibility in conformation adapt-

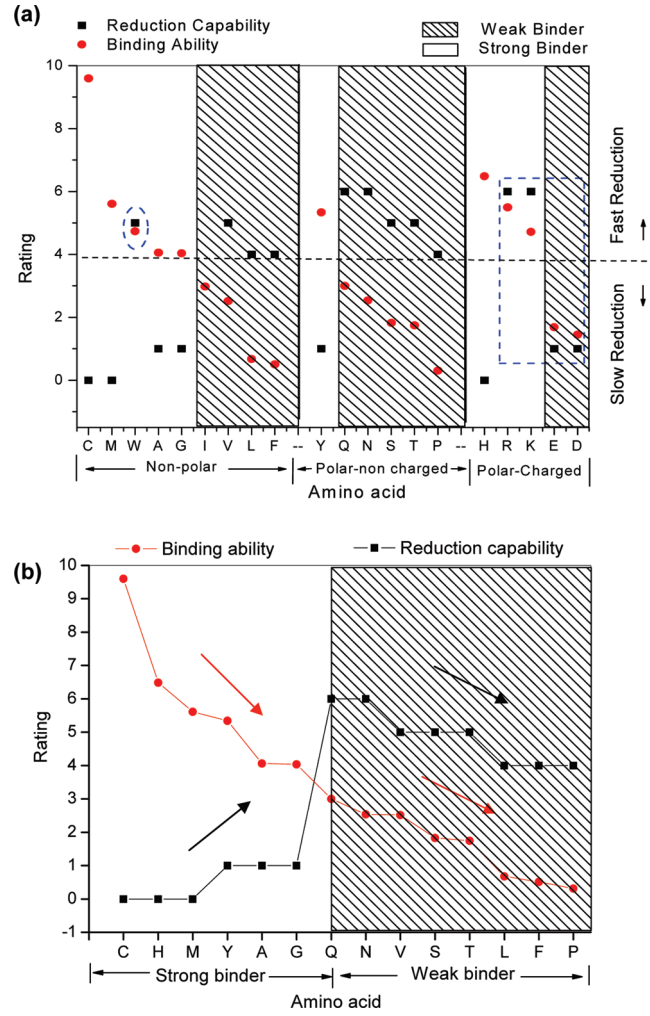

Figure 4. (a) Reduction (black squares) and binding (red circles) ratings for the 20 natural α-amino acids-interdigitated peptides. Reduction rating was based on scheme I in Figure 2, while binding rating was based on the normalized fractional surface coverage on gold in Figure 3c. A scaling factor of 3 was applied to the latter to improve visualization. (b) Correlation between reduction rating and binding rating (except for charged peptides). The shaded areas are used to aid comparison between the weak and strong binders.

ability, thereby causing the reactive side chains of the peptide (both of P and H) to interact the least optimally with the gold surface, resulting in the weakest binding. These results imply that the binding affinity of an individual amino acid residue in a peptide sequence is governed by its reactive side group as well as by its contribution to the peptide's adaptability to conformations favorable for adsorption on gold.

Peptide Sequence−Activity (Crystal Growth) Relationship. While the nearest-neighbor effects in peptides on chloroaurate reduction and binding to metallic gold were discussed separately in previous sections, these two functions of interdigitated peptides are indeed interrelated, and further insights may be gained by examining them side-by-side. The overall mapping of the experimental results in Figure 4a reveals a number of trends: (1) In general, strong binders (i.e., binding rating[47] > 3)

(47) For ease of visualization, the binding rating, which is the equilibrium surface coverage of the peptide in question on gold normalized by the equilibrium surface coverage of QHQHQHQ, was multiplied by a factor of 3 (Figure 3c).

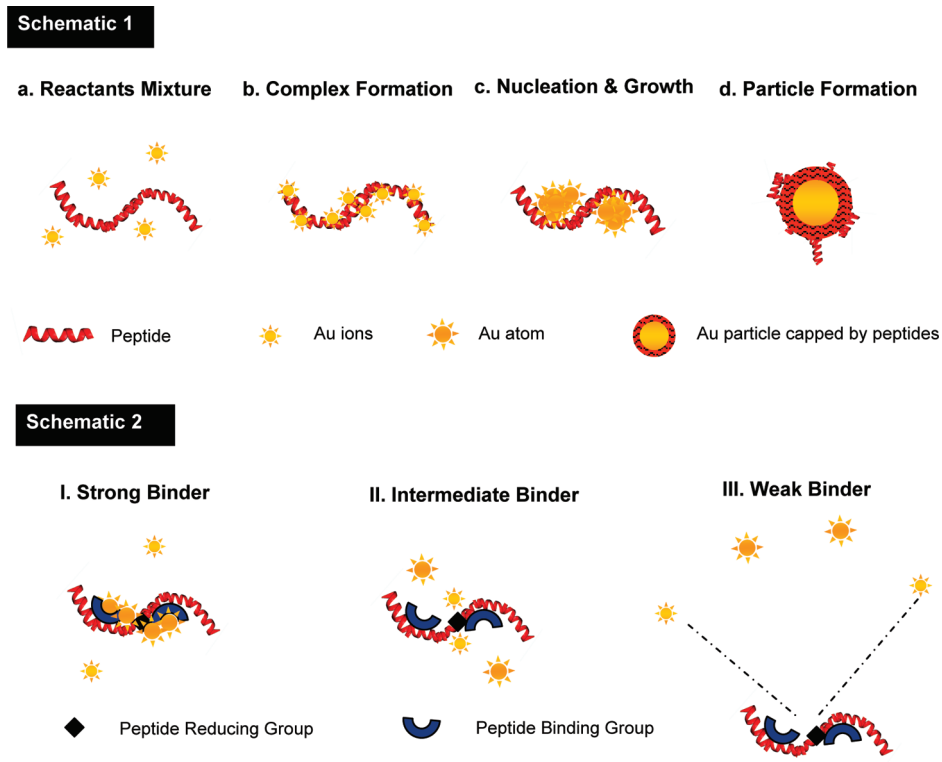

Figure 5. Schematic 1: A proposed model for the peptide synthesis of gold nanoparticles in the aqueous solution. (a) The reactant mixture of peptides and chloroaurate ions. (b) The formation of peptide−$AuCl_4^-$ complexes. Strong complexes inhibited the subsequent reduction to Au(0). (c) Reduction facilitated by peptides to form Au atoms for nucleation. (d) Growth of nuclei into crystalline particles by addition of more Au atoms from the solutions or by fusion with other nuclei. Schematic 2: The molecular interactions between peptide and Au ions and peptide and gold atoms which determined the reactivity of the peptide for reduction. The reducing residues of the peptide were sandwiched by the (I) strong, (II) intermediate, and (III) weak Au-binding residues, respectively.

tend to have low reduction capability (reduction rating[48] < 4), while weak binders (i.e., binding rating < 3) tend to have high reduction capability (reduction rating > 4). Since tryptophan by itself is a strong reducing agent, the interpretation of results from the reducing peptide W_7 requires caution. The moderation of the reduction capability of W when it was present as the W_7 homopeptide could be attributed to the relatively strong binding affinity of W to the gold surface formed upon reduction, which resulted in a *self-regulation* of the activity of W in chloroaurate ion reduction. (2) This, however, was not the case among the charged polar amino acid residues when they were connected in a peptide sequence, where the reduction capability was good for the strong binders (R, K) and poor for the weak binders (E, D). The effect of the peptide net charge on the reduction of the chloroaurate ions to elemental gold was therefore considered (Table S3, Supporting Information). The analysis suggested that positively charged peptides (RWRWRWR and KWKWKWK) were favorable for the reduction reaction because of their ability to bring the chloroaurate anions closer for reduction, while the charge repulsion between negatively charged peptides (EWEWEWE and DWDWDWD) and chloroaurate anions frustrated the reduction reaction. (3) *Aside from the charged peptides*, a closer examination of the mapping results within the same binding affinity group (strong or weak) revealed some classifiable trends between reduction capability and binding affinity (Figure 4b). The reduction capability of the strong binders was found to increase with the decrease in their binding affinity, whereas the amino acid residues classified as weak binders displayed a positive correlation between these two properties. Considered together, these two correlations suggest that increased binding strength improves the reduction reaction up to a point whereafter further increase in binding actually would suppress gold nanoparticle formation.

A model for the peptide synthesis of gold nanoparticles may then be proposed to rationalize the experimental observations (schematic 1 in Figure 5). Upon mixing the gold precursor and the peptide in an aqueous solution, the extent of complexation between the peptide and metal ions determines whether the reduction reaction could occur. In the mixture study, the strong complexation between the metal ions and amino acids in the C−W, H−W, and M−W mixtures rendered the metal ions inactive for reduction. This was also the case for peptides containing these strong metal-ion chelators (e.g., CWCWCWC, HWHWHWH, and MWMWMWM), where no reduction was detectable even though the peptides were interdigitated with the strongly reducing W residues. In particular, a white precipitate every bit as "organic" as an aggregated peptide was formed using the C−W interdigitated peptides. The precipitate was most likely peptides cross-linked by the chloroaurate ions. Since the C, H, and M residues with Au-ion-chelating groups also formed peptides with the strongest binding to the Au surface, it is reasonable to postulate that the degree of complexation between the metal ions and amino acids would follow the trend shown in the peptide binding study. Therefore, chloroaurate reduction was possible for W−X interdigitated peptides where X does not chelate strongly with the Au ions, although some degree of complexation would be advantageous to initiate the reduction reaction.

Even if the reduction reaction could be initiated, the rate of reaction would be determined by the reduction capability of the peptide, which is clearly sequence dependent (Schematic 2

(48) Based on the rating scheme I in Figure 2 using XWXWXWX peptide.

in Figure 5). It was found that the presence of a relatively strong binder (e.g., Y, G, or A) in W−X interdigitated peptides would lower the reduction capability. This could be understood as an entropy effect in thermodynamic terms. In principle, the unreacted peptide in the reduction reaction should remain extended and available for further reactions. However, the strong binder-containing peptides could easily make multiple contacts with the Au surface initially formed. This corresponds to an entropy penalty (decrease) that resulted in a less negative change in the Gibbs free energy ($\Delta G = \Delta H - T\Delta S$) for reduction, and hence a lower reactivity for the peptide.[49] The ability of the peptide to bring the chloroaurate anions into close vicinity for reduction is another consideration. As shown previously, the charge repulsion between negatively charged peptides and chloroaurate anions was adversarial to reduction. Similarly, the reason the weak binder (e.g., L, F, and P)-containing peptides did not show good reactivity for reduction could also be their poor ability to bring the chloroaurate anions into close proximity for reduction. All in all, the model suggests that an intermediate binding affinity of peptide for metal *ions* as well as for metal *surfaces* would be best for nanoparticle formation, as such a peptide would possess adequate reducing power and the ability to bring the chloroaurate ions closer to the reduction sites without excessive chelation which inactivates the metal ions. As a result, the careful selection and programming of binding amino acid residues into a reducing peptide sequence could confer properties that allow for a certain degree of reduction kinetics control in different stages of nanoparticle formation from initial complex formation to nucleation and growth of the nanoparticles.

Peptide Design Principles in Tuning Reduction Kinetics for Particle Size and Shape Control. The findings from the above kinetic and binding studies could be used as the first basis for designing peptides with adjustable reducing power to control the crystal growth of nanoparticles. As a proof of concept, we designed a series of peptides with the same overall amino acid composition but different sequences to examine more closely the effects of neighbors on the reduction capability of reducing residues in a peptide sequence. The test peptides were assembled from a strong reducing residue (W), a strong binder (G), and a weak binder (L). Figure 6 shows that the kinetics of gold nanoparticle formation was greatly affected by the binding strengths of the nearest neighbors to the WW (W_2)[50] reducing sequence: G**L**WW**L**G > G**L**WW**G**L ≈ L**G**WW**L**G > L**G**W-W**G**L. The reducing power of W_2 was down-regulated by the strong binder G and up-regulated by the weak binder L in the nearest-neighbor positions. It was also noted that the left and right positioning of the up- and down-regulators in the peptide sequence did not affect the reduction kinetics significantly. In the context of the discussion that follows, the terms "strong binders"/"down-regulators" and "weak binders"/"up-regulators" will be used synonymously. The results from the W_2GL series of peptides demonstrate clearly the important role of the nearest neighbors. Hence, the reducing power of a peptide could be tuned by placing up- or down-regulators immediately next to the reducing residues in the peptide sequence. The next challenge would be to apply these basic rules to the morpho-synthesis of metal nanoparticles via kinetic control.

Previously, Brown et al. identified two sequences (SEKL- and GASL-containing repeats) in the gold-binding polypeptides from *Escherichia coli* which could exercise shape-directing function in gold crystal growth.[31] However, relatively large gold nanoplates (500−1000 nm) were obtained because of the slow rate of the reduction reaction. This is not surprising since these gold-binding sequences are large (>100-mer) and complex and contain a large number of strong binders which are rate down-regulators. On the basis of our understanding of the peptides' sequence−activity for reduction kinetics control, we designed a number of short multifunctional peptides for the synthesis of *small* gold nanoplates by assembling a gold precursor reduction sequence, a reduction rate modulation sequence, and a particle shape-directing sequence into one. In the design, a homodipeptide sequence (i.e., WW, YY, and FF) that contains amino acid residues with different reduction capabilities (W > Y > F) and binding strengths (Y > W > F) was sandwiched between two shape-directing sequences to enable simultaneous size and shape control by manipulating the gold precursor reduction kinetics. Peptide SEKLGASL, which represents the intrinsic activity of the shape-directing sequences without extraneously introduced reducing residues and rate modulators, was used as the control for the comparative experiments. Kinetic plots in Figure 7a−d (left) show that the reduction rates decreased in the following order: SEKL**WW**GASL > SEKL**FF**GASL > SEKLGASL (*control*) > SEKL**YY**GASL. As expected, the W_2 peptide synthesis of gold nanoparticles had the fastest reduction kinetics because of the strong reduction capability of W_2 and limited self-regulation effect.[51] The reduction capability of the F_2 peptide was next. Here, the reduction capability of F was up-regulated (F_2 > F) by its relatively weak binding strength. The strong binding strength of Y, on the other hand, down-regulated its own reduction capability in the Y_2 sequence (Y_2 < Y). Here, the self-regulation effect took center stage because Y has stronger binding capability than reduction capability. The corresponding TEM images in Figure 7b−d (right) display the expected decrease in the size of the gold nanoplates with the increase in reduction kinetics delivered through the use of different reducing residues and rate regulators.

Two additional peptides were then designed by switching the order of the shape-directing sequences about the sandwiched

(49) Since W was used as the common reducing residue in the W−X peptide sequence, the major difference between the reduction capabilities of the 20 interdigitated peptides should be contributed by the X residue. However, it was found that the reduction capability of a W−X peptide is not a linear sum of the capabilities of its amino acid constituents. For example, tyrosine (Y), which showed fairly good reduction capability on its own, actually downgraded the reactivity of W more so than other amino acids when it was incorporated as the W−Y sequence (Figure 2b). This result shows that the intrinsic reduction property of an amino acid (X) is less influential than its binding affinity in affecting the overall reduction performance of an interdigitated peptide. This is even true when the strongest reducing amino acid (i.e., W) was used as the common interdigitated residue. Hence, the ΔH contribution from the intrinsic reduction capability of X is minor compared to the ΔS contribution, and the ΔG in the peptide reduction of metal precursor is controlled by the entropy effect.

(50) We discovered that conjoining two identical amino acids (e.g. W_2) in a peptide sequence would elevate the more prominent feature (e.g., for W it is reduction capability) of that particular amino acid. Hence, a W_2 sequence would enhance the reduction capability of the peptide (relative to the interspersed presence of W in the peptide) to allow the reaction to be completed within a reasonable time period. The self-regulation effect in the W_2 dipeptide was quite minimal compared to that in W_7. This is because the smaller number of gold-binding sites (two vs seven) would not impose a strong compensational effect on gold ion reduction.

(51) We have also carried out experiments in which a single amino acid residue (W, Y, or F) was inserted between the shape-directing sequences. The self-regulation effect was absent in this case, and the reduction rate follows the reduction capability of the inserted residue, decreasing in the following order: SEKL**W**GASL > SEKL**Y**GASL > SEKL**F**GASL. Hence, self-regulation in a homodipeptide sequence would elevate the more prominent feature of the amino acid involved (e.g., for W, it is the reduction capability).

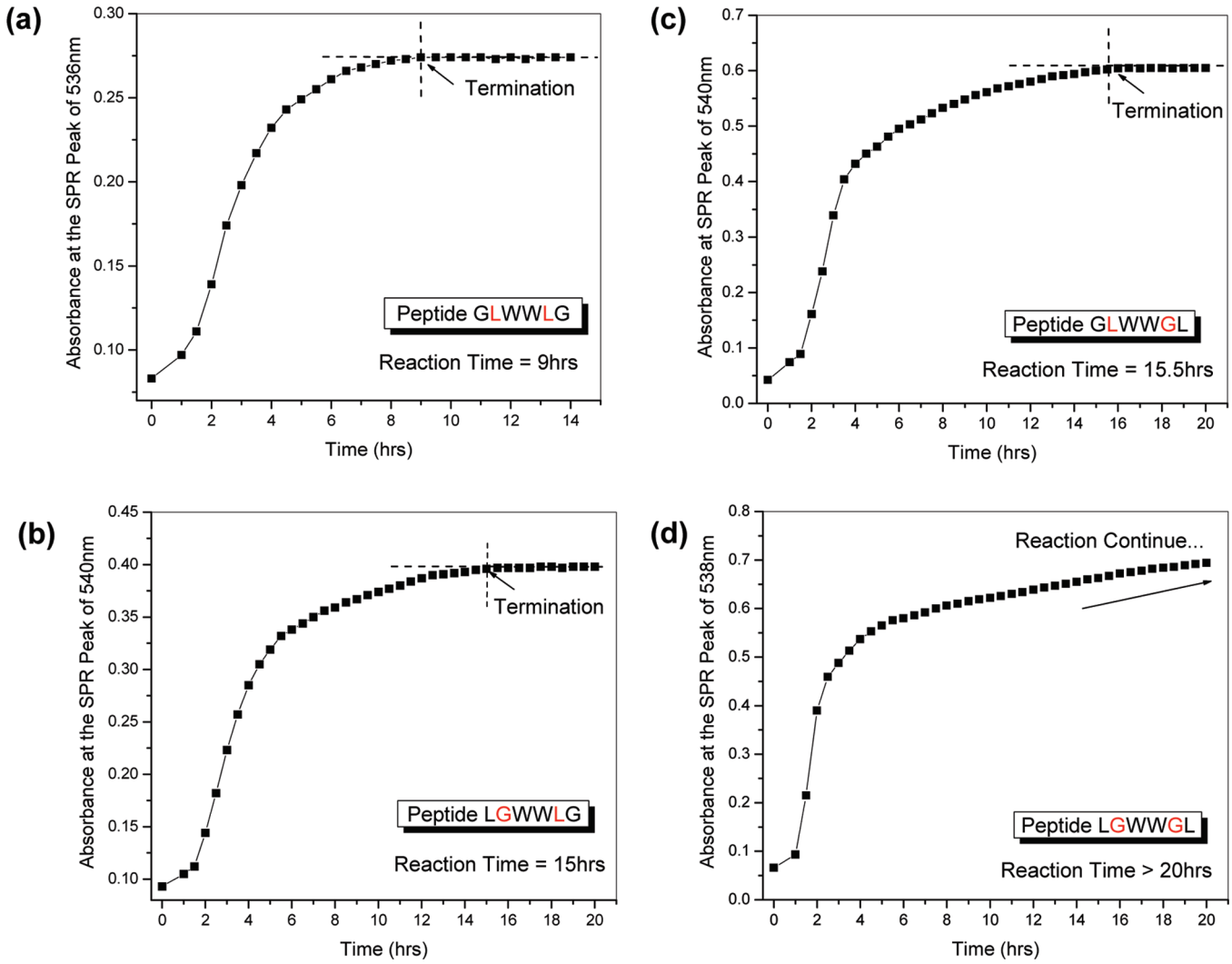

Figure 6. Comparison of the kinetics of reduction in peptide synthesis of gold nanoparticles using peptides of the same amino acid composition but different sequences: (a) GLWWLG > (b) LGWWLG ≈ (c) GLWWGL > (d) LGWWGL.

dipeptide (i.e., ***SEKL***WW***GASL*** (SL-10) vs ***GASL***WW***SEKL*** (GL-10)). The results in Figure 7e show that swapping the shape-directing blocks had significantly affected the reduction kinetics as well as the morphology (i.e., size and shape) of the particles formed. A closer examination of the amino acid nearest neighbors to the W_2 sequence revealed that the reduction rate of the W_2 sequence was increased in GL-10 by the placement of two reduction rate up-regulators (L, S). Modification of the W_2 activity by one up-regulator (L) and one down-regulator (G) in the SL-10 peptide resulted in a slower reaction rate than GL-10. The fast reduction kinetics witnessed upon adding the GL-10 peptide solution to the chloroaurate solution led to the formation of very small gold nanospheres. While the high reduction rate favored the formation of smaller particles, it suppressed the anisotropic growth into nanoplates. In this case, the reducing power of the W_2 sequence promoted by the nearest-neighbor effect overshadowed the shape-directing effect of the SEKL and GASL sequences.

In general, anisotropy in nanoparticle product is caused by the asymmetric adsorption of capping molecules (e.g., peptides) on different crystallographic planes of the nuclei. Because peptides were also used here as the reducing agent, the reaction kinetics therefore affected both the size and the shape of the nanoparticles formed. Generally, morphosynthesis of gold nanoparticles is a kinetically controlled process where a slow growth environment favors the selective adsorption of the capping molecules on the nuclei and the development of anisotropy. The selectivity is lost under a high growth condition. Such kinetic effects have been experimentally confirmed (Figure 7a−d). Hence, an increase in the reduction kinetics (through the use of different reducing residues and rate regulators with the same shape-controlling sequence) would decrease the particle size and the proportion of anisotropic shapes in the product. Figure 7e, in particular, shows that, under extremely fast reduction, only small nanospheres would be formed despite the presence of a shape-controlling sequence. This is because the specific adsorption of peptide on the gold nuclei was not sufficiently fast in this case to compete with the rapid addition of gold atoms from the reduction reaction. The selective adsorption process therefore could not proceed. Taken together, the experimental results could be explained by a mechanism where the difference in reaction kinetics and the competition between the reduction and binding functions of peptide determine the shape and size of the nanostructures formed.

From the experimental results above, a few guiding principles may be concluded for the peptide morphosynthesis of gold nanoparticles: (1) a shape-directing sequence (e.g., SEKL and GASL) must be present in the peptide to induce the formation of the desired shape; (2) the peptide design should factor in a strong reducing sequence (e.g., W_2) to accelerate the reduction

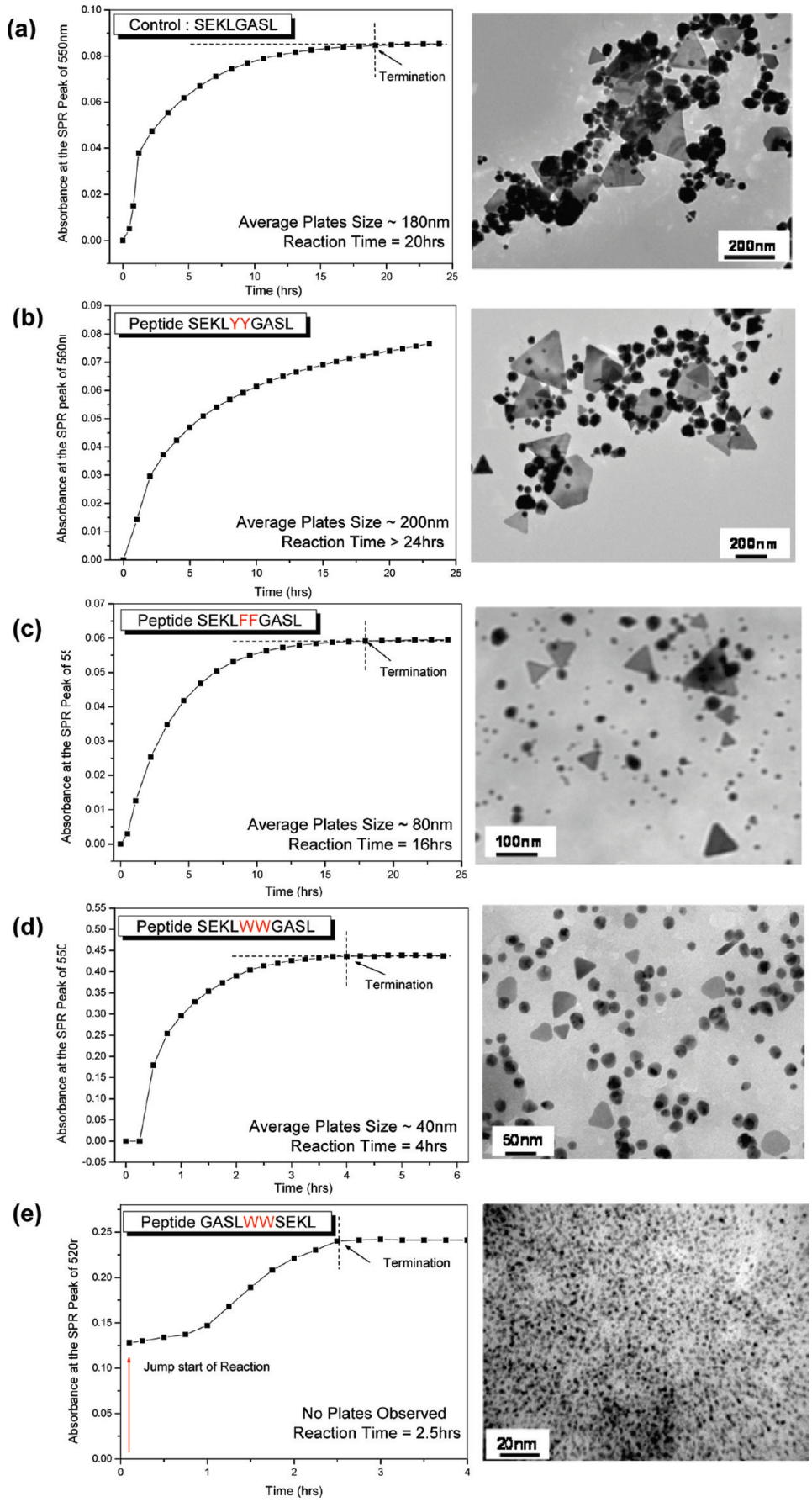

Figure 7. TEM images (right) and the corresponding reduction kinetics of peptide synthesis of gold nanoparticles (left) using multifunctional peptides: (a) SEKLGASL (*control*), (b) SEKLYYGASL, (c) SEKLFFGASL, (d) SEKLWWGASL, and (e) GASLWWSEKL.

kinetics to form smaller gold nanoplates; and (3) reduction rate regulators may be placed next to the reducing sequence for added effects. However, it is important to select and position the amino acid residues strategically in the overall design of multifunctional peptides (e.g., SL-10 vs GL-10) to enable good size and shape control of the product nanoparticles via kinetic effects.

Conclusions

In summary, the formation of metal nanoparticles by short peptides is primarily determined by two basic functionalities of the amino acid residues: reducing capability for metal ions and capping (binding) capability for the nanoparticles formed. The peptide sequence−activity relationships that have been established here can be used as the basis for designing peptides to simultaneously deliver shape and size control in a gold nanoparticle synthesis. Contrary to the common practice of relying on reaction macroenvironment adjustments (e.g., pH, temperature and reactant concentration) for kinetic control, the peptide synthesis of metal nanoparticles delivers more precise kinetic control at the reaction microenvironment level by dialing in different amino acid sequences for the right combination of reducing, capping, and morphogenic functions. However, it is noteworthy to mention that, as the peptide chain becomes longer, the increasing complexity of the peptide sequence and the increasing possibility for structure and conformation variations may also contribute to the overall functions of the peptides. We hope that with the continuing efforts toward understanding the peptide sequence−crystal growth relationship at the amino acid level, a "green" biomimetic synthesis may eventually be possible where rationally designed multifunctional peptides are used to produce nanomaterials with prescribed geometrical features depending on the needs of the application.

Experimental Section

Materials and Instrumentation. Hydrogen tetrachloroaurate(III) trihydrate ($HAuCl_4 \cdot 3H_2O$, ≥99.5%) and the 20 natural α-amino acid (≥98.5%) were purchased from Sigma-Aldrich Chemicals. Tryptophan-interdigitated peptides, XWXWXWX, and histidine-interdigitated peptides, XHXHXHX, where W is tryptophan, H is histidine, and X is one of the 20 naturally occurring amino acids (e.g., AWAWAWA for alanine-tryptophan interdigitated peptide and AHAHAHA for alanine-histidine interdigitated peptide), were supplied by Research Biolabs Pte Ltd. (Singapore) at purity ≥90.0% (Tables S3 and S4, Supporting Information). Peptides GLWWGL, LGWWLG, LGWWGL, and GLWWLG were supplied by Research Biolabs Pte Ltd. (Singapore). Peptides SEKLGASL, SEKLFGASL, SEKLYGASL, SEKLWGASL, SEKLFFGASL, SEKLYYGASL, SEKLWWGASL, and GASLWWSEKL were purchased from GL Biochem Ltd. (Shanghai). The purity of these custom-made peptides was ≥90.0% (Table S5, Supporting Information). The HBS-EP buffer (10 mM HEPES pH7.4, 150 mM NaCl, 3 mM EDTA, and 0.005% (v/v) surfactant P20) and the gold sensor chips for a Biacore 2000 surface plasmon resonance spectrometer were supplied by Biacore AB (Uppsala, Sweden). All chemicals and materials were used as received without further purification. Ultrapure water (18 MΩ, prepared using a Millipore Elix 3 purification system) was used as the universal solvent unless indicated otherwise. UV−visible spectroscopic measurements were carried out on a Shimadzu UV-2450 spectrophotometer at 1 nm resolution. They were used to follow the progress of reaction upon mixing the amino acid/peptide solution with the gold precursor solution ($HAuCl_4$). The as-synthesized gold nanoparticles were imaged by a JEOL JEM-2010 transmission electron microscope operating at 200 kV. All samples for microscopy were prepared by dispensing 10 μL of the nanoparticle solution onto a 3 mm carbon-coated copper grid, followed by drying in vacuum at room temperature.

Amino Acid and Peptide Syntheses of Gold Nanoparticles. The amino acid synthesis of gold nanoparticles was carried out in aqueous mixtures with 0.7 mM amino acid and 0.1 mM $HAuCl_4$. The amino acid mixture-synthesized gold nanoparticles were prepared in solutions with 0.1 mM $HAuCl_4$ and a 0.7 mM concentration of an amino acid mixture containing W and one of the 20 naturally occurring amino acids (X) in a 3/4 ratio. Tryptophan-interdigitated peptides, XWXWXWX, with the same overall amino acid compositions and W/X ratio as the amino acid mixtures were used to examine the proximal effects of neighbors (X) on the reduction capability of W in a peptide sequence. W−X interdigitated peptide-synthesized gold nanoparticles were prepared by adding 200 μL of 0.2 mM $HAuCl_4$ to 200 μL of a 0.2 mM concentration of dissolved peptide, yielding 0.1 mM $HAuCl_4$ and 0.1 mM peptide. The kinetics of chloroaurate ion reduction by the custom-designed peptides was studied in 0.2 mM $HAuCl_4$ and a 0.4 mM concentration of one of these peptides: GLWWGL, LGWWLG, LGWWGL, and GLWWLG. The morphosynthesis of gold nanoplates was performed in 0.1 mM $HAuCl_4$ and a 0.3 mM concentration of one of the multifunctional peptides: SEKLGASL, SEKLFFGASL, SEKLYYGASL, SEKLWWGASL, and GASLWWSEKL. Ultrapure water was used as the sole solvent for most of the amino acids and peptides except for a few in the form of W−X interdigitated peptides (i.e., X = W, M, L, F, C, V, and Y), which required the presence of DMSO as a cosolvent. In such cases, the peptide was first dissolved in 100 μL of DMSO, and then water was added to the desired concentration (0.2 mM in a final volume of 500 μL).

Measurements of Binding Affinity by Surface Plasmon Resonance Spectroscopy. The adsorption of histidine-interdigitated peptides, XHXHXHX, on Au was measured by a Biacore 2000 SPR spectrometer using Biacore BR-1005-42 Au sensor chips. For the measurements, the peptide was first dissolved in HBS-EP buffer to form a 2 mg/mL stock solution. The stock solution was then diluted to obtain peptide solutions with concentrations from 0.05 to 1.00 mM. A flow rate of 2 μL/min was used throughout. The measurement commenced by establishing a baseline with the flowing HBS-EP buffer solution. The port was then switched over to the peptide solution, and flow continued until equilibrium was re-established. All measurements were carried out at 25(±0.1) °C maintained by the temperature controller of the SPR system.

Acknowledgment. This work was supported by Singapore−MIT Alliance (SMA) program and the Academic Research Grant R-279-000-204-112 from the Ministry of Education (Singapore). Y.N.T. acknowledges SMA for a research scholarship. The authors thank S. T. Lim (National University of Singapore) for assistance with SPR measurements.

Supporting Information Available: Table S1, reduction of $HAuCl_4$ by amino acids (X) and amino acid mixtures (W−X) with tryptophan (W) as the common constituent; Figure S1, kinetics of W-interdigitated peptide (XWXWXWX) synthesis of gold nanoparticles; Figure S2, measurement of H-interdigitated peptides (XHXHXHX) adsorption on gold surface by SPR spectroscopy; Table S2, binding constant K_A and maximum binding capacity R_{max} of H-interdigitated calculated from SPR data; Tables S3−S5, purity and selected physical properties of W-interdigitated peptides, H-interdigitated peptides, and multifunctional peptides used for the proof of design principles. This material is available free of charge via the Internet at http://pubs.acs.org.

JA907454F